Light Water Reactor Sustainability Program

Environmentally Assisted Fatigue in Light Water Reactor Environment

Yiren Chen, and Bogdan Alexandreanu
Nuclear Science and Engineering Division, Argonne National Laboratory

August 2024

U.S. Department of Energy
Office of Nuclear Energy

Environmentally Assisted Fatigue in Light Water Reactor Environment

Nuclear Science and Engineering Division

Environmentally Assisted Cracking in Light Water Reactor Environment

prepared by
Y. Chen and B. Alexandreanu
Nuclear Science and Engineering Division, Argonne National Laboratory

August 2024

ABSTRACT

This report summarizes the Environmentally Assisted Fatigue (EAF) research conducted at ANL under the US DOE Light Water Reactor Sustainability (LWRS) program. Starting from a rich background in theoretical and experimental EAF, ANL previously developed an approach to evaluate fatigue performance of reactor materials in light water reactor environments with the correction factor F_{en}. The approach was based on a large body of experimental work performed at ANL and elsewhere, and was consistent with American Society of Mechanical Engineers (ASME)'s methodology governing the design and construction of reactor components. In recent years, the program was focused on component fatigue prediction and made several major and fundamental contributions in this area. These accomplishments help meet the needs identified by the industry concerning component level fatigue predictions in complex, transient conditions. The main contribution of the ANL program involved the development of a system-level model for estimating residual strain and life of nuclear reactor coolant system components under connected-system-thermal-mechanical boundary conditions. The goal was to predict the stress hotspots, strain residuals, strain amplitudes and the resulting fatigue lives. Thermal-mechanical stress analysis was performed considering thermal stratification and a design-basis reactor loading cycle. Based on the finite element (FE) model results, the strain residuals, strain amplitudes and resulting fatigue lives of reactor coolant system (RCS) components were predicted. The results show that some of the RCS components can have significantly different strain amplitudes, residual strain, and fatigue lives, despite having similar geometry and material. In addition, the simulated component-level strain profile can guide the selection of appropriate test inputs for conducting laboratory-scale EAF tests. Building upon the system-level model, ANL developed a digital twin (DT) framework to predict the structural states and associated fatigue life of components in real-time. This framework is a comprehensive system designed to predict the structural states and fatigue lives of reactor components. It includes multiple models and integrates artificial intelligence (AI), machine learning (ML), and FE based modeling tools to evaluate the structural states and fatigue lives.

TABLE OF CONTENTS

LIST OF FIGURES

LIST OF TABLES

ACKNOWLEDGMENTS

1. Introduction

Metal fatigue is a degradation mechanism of structural materials subjected to repeated stress or strain cycles. Under cyclic loading, metallic materials can sustain cracking or even failure when the stress is well below the value considered "safe" for static loads [1]. Microscopic damage and irreversible deformation can accumulate in metals, leading to fatigue damage or cracking. Figure 1 shows an example of a fatigue crack initiated from a smooth sample's surface under cyclic loading, moving toward the interior. In light water reactors (LWRs), structural components can certainly experience repeated load cycles caused by mechanical vibrations and operational transients of pressure and temperature during service, making fatigue damage a critical concern for both reactor design [2] and operation [3]. To manage this form of material deterioration, fatigue analysis is performed during the design phase of LWRs to predict the fatigue lives of reactor components. The American Society of Mechanical Engineers (ASME) Boiler and Pressure Vessel Code (BPVC), Section III, Subsection NB establishes rules for design and construction of Class 1 components (pressure retaining components and piping) for nuclear power plants. Applications of these rules involve using fatigue design curves, stress analysis, and strain-life (ε-N) or stress-life (S-N) approaches to estimate the number of cycles a component can endure before failure.
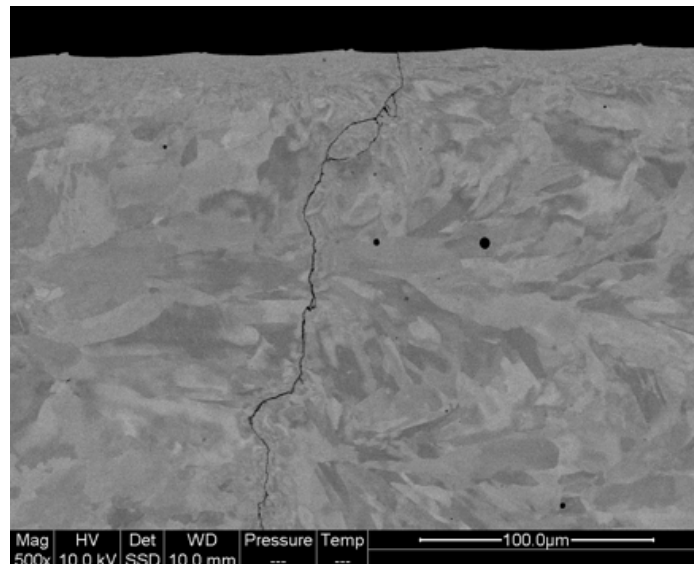
Figure 1. A fatigue crack initiated from the surface of a Type 316L SS sample

Fatigue damage can be categorized into high-cycle fatigue and low-cycle fatigue [1]. While the underline mechanism of these forms of fatigue damage is the same, high-cycle fatigue typically involves a very large number of cycles and relatively low stresses. The material's elastic behavior dominates this form of fatigue, and the primary concern is the endurance limit – a stress level below which fatigue failure is unlikely. For low-cycle fatigue however, materials experience significant plastic strains. As a result, low-cycle fatigue is often associated with higher stress levels and much lower numbers of cycles to failure compared to high-cycle fatigue. For LWR components subjected to varying operating loads and temperatures, low-cycle fatigue is the most

common fatigue mode to be considered. Since detailed information on cyclic stress-strain behavior is important for low-cycle fatigue, fatigue analysis based on strain-controlled tests are typically used.

During in-service operation, structural materials experiencing cyclic loads are often exposed to high-temperature reactor coolant at the same time in LWRs. Stress corrosion cracking (SCC) and environmentally assisted fatigue (EAF) are the fundamental micro-mechanisms operating in the deaerated water environments at elevated temperatures [4]. Several recent reviews summarizing the effects of LWR coolant on the cracking and fatigue performance of reactor materials can be found in literature [5][6]. Reactor vessels, which are often constructed with low-alloy steels (LAS), are of the primary concern. Fatigue damage can weaken the structure by introducing flaws, and LWR water environment can facilitate and accelerate this process. Along with the embrittlement of low-alloy steels resulting from thermal aging and neutron irradiation, fatigue damage can challenge the long-term integrity of the LWR pressure vessels.

In addition to the reactor pressure vessel (RPV), reactor coolant piping and vessel head penetrations are also part of the primary pressure boundary. These components are commonly made of austenitic SSs or Ni-based alloys, and are welded to the reactor pressure vessel with dissimilar metal welds as illustrated in Figure 2. Numerous studies have been carried out in recent years focusing on thermal aging and SCC performance of these materials and welds in service environments. Environmentally assisted fatigue can be crucial for the service performance of these reactor components, not only because of the pervasive nature of fatigue damage, but also because of the synergies between fatigue and other forms of deterioration mechanisms. Premature failures originated from or propagated under cyclic loads have been reported [3]. A better understanding of fatigue and EAF behaviors are crucial for the safety and long-term operation of LWRs.
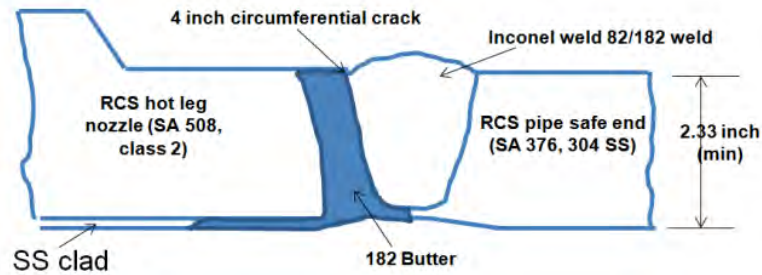
Figure 2. A schematic of RPV nozzle to hot-leg pipe weld

2. Fatigue Analysis and F_{en} Factor

The method used in the ASME Code for developing fatigue design curve with strain-life data was pioneered by Langer [7] in the 1950s. Based on Coffin's work [8], the fatigue behavior of a wide range of materials follows a relationship,

$$\sqrt{N} * \varepsilon_p = C \tag{1}$$

where N is fatigue life, ε_p is plastic strain range, and C is a material constant which can be conservatively taken as one half of the true fracture strain in a tensile test ε_f [9]. Since the fracture strain can also be expressed in the reduction of area (RA),

$$\varepsilon_f = \ln\left(\frac{100}{100-RA}\right) \tag{2}$$

the stress amplitude, S_a, in cyclic loading can be written as

$$S_a = E * \frac{\varepsilon_p}{2} + E * \frac{\varepsilon_e}{2} = \frac{E}{4\sqrt{N}} * \ln\frac{100}{100-RA} + \Delta S \tag{3}$$

where E is elastic modulus, ε_e is elastic strain range, and ΔS is stress amplitude which can be conservatively taken as the endurance limit, S_e.

$$S_a = \frac{E}{4\sqrt{N}} * \ln\frac{100}{100-RA} + S_e \tag{4}$$

Fit the fatigue data of a material to equation (4), the material's fatigue behavior can be described. With this approach, ASME Code best-fit curves at room temperature are obtained for carbon steels,

$$S_a = \frac{59,734}{\sqrt{N}} + 149.2 \tag{5}$$

for low-alloy steels,

$$S_a = \frac{49,222}{\sqrt{N}} + 265.4 \tag{6}$$

and for austenitic stainless steels (SSs) and other nickel-chromium-iron alloys,

$$S_a = \frac{58,020}{\sqrt{N}} + 299.9 \ . \tag{7}$$

These formulas can also be expressed in the form of fatigue life (N) vs. strain amplitude (ε_a) as,

$$\ln(N) = A - B \ln(\varepsilon_a - C) \tag{8}$$

where A, B, and C are constant. The expressions for carbon steels, low-alloy steels, and SSs are shown in Eq. (9), Eq.(10), and Eq.(11), respectively.

$$\ln(N) = 6.726 - 2 * \ln(\varepsilon_a - 0.072) , \tag{9}$$

$$\ln(N) = 6.339 - 2 * \ln(\varepsilon_a - 0.128) , \tag{10}$$

$$\ln(N) = 6.891 - 1.920 * \ln(\varepsilon_a - 0.112)^1. \tag{11}$$

Since these fitting curves are developed with strain-controlled tests on small, polished samples, they must be adjusted to account for other effects not captured by the small-sample tests. The first adjustment is to account for the mean stress effect. Since the fatigue curves are established with completely reversed stress cycles through zero, a mean stress would reduce the endurance limit at the high-cycle end of the curve. This effect can be accounted for with the modified Goodman relationship [7],

$$S'_a = S_a * \frac{\sigma_u - \sigma_y}{\sigma_u - S_a} \qquad \text{for } S_a < \sigma_y, \tag{12}$$

$$S'_a = S_a \qquad \text{for } S_a > \sigma_y, \tag{13}$$

where S'_a is the adjusted stress amplitude, σ_y and σ_u are the yield and ultimate strength, respectively, in a tensile test. At the low-cycle end, a mean stress has little or no effect on the fatigue life.

Following the mean-stress adjustment, the fatigue curves are further reduced by one of the two factors on stress (a factor of 2) and on life cycles (a factor of 20), whichever is more conservative. This adjustment is intended to capture other effects not accounted for in the small sample tests. The factor of 20 on life cycles is originated from three subfactors -- scatter of data (2.0), size effect (2.5), and surface finish (4.0) [14]. With these adjustments, fatigue design curves can be obtained for different materials. Note that these curves are for in air applications, and the effects of LWR coolant on fatigue performance are not considered [2].

In an effort to evaluate the effects of LWR coolant on fatigue, Chopra and coworkers reviewed and analyzed the existing fatigue data for carbon and low-alloy steels, SSs, and Ni-Cr-Fe alloys in air and in LWR environments. The results were summarized in the initial NUREG-6909 report [15] and later in its revision [16]. For the fatigue design curves in air, significant effort was made to assess the subfactors to be applied on life cycles. The effects of data scatter and materials variability, size effect, surface finish, and loading history on the fatigue behavior were assumed to be independent from each other and were evaluated separately. The resulting subfactors for

---

[1] Note that ASME Code prior to the 2009 Addenda is given as ln(N)=6.954-2*ln(ε_a-0.167).

each variable along with the subfactors recommended in ASME Code are shown in Table 1. Note that a range, rather than a fixed value, was provided for each subfactor.

Table 1. Subfactors for fatigue design curve on life cycles

Subfactor	ASME Code Section III	NUREG-6909, Rev 1
Data scatter and material variability	2.0	2.1-2.8
Size effect	2.5	1.0-1.4
Surface finish	4.0	1.5-3.5
Loading history	-	1.0-2.0
Overall reducing factor	**20**	**3.15-27.4**

With the EAF data from ANL and other sources, similar analysis was performed with key parameters, such as temperature, strain rate, dissolved oxygen (DO) content in water, and sulfur content in steels [15]. The EAF data were fitted to a modified version of Eq. (8)

$$\ln(N) = A' - B' \ln(\varepsilon_a - C') + DS^*T^*O^*\dot{\varepsilon}^* \,, \tag{14}$$

where A', B', C', and D are material constants, and $S^*, T^*, O^*,$ and $\dot{\varepsilon}^*$ are the transformed parameters of sulfur content, temperature, DO level, and strain rate, respectively. Threshold and saturation values are assumed for the transformed parameters. Another reducing factor, F_{en}, can then be established to account for the effects of LWR environments. The F_{en} is defined as the ratio of the fatigue life in air at room temperature, $N_{RT\text{-air}}$, to the fatigue life in water at the service temperature, N_{water}. In Eq. (14), A', B' and C' represent the same characteristics of the ε-N curve as A, B, and C do in Eq. (8). Assuming the slopes of ε-N plot and the fatigue limits are the same for both in-air and LWR-environment models, we have B=B' and C=C'. The F_{en} can then be written as

$$\ln(F_{en}) = \ln(N_{RT-air}/N_{water}) = A - A' - DS^*T^*O^*\dot{\varepsilon}^* \,. \tag{15}$$

Fit the environmental fatigue data to the expression [15], F_{en} is obtained for carbon steels,

$$F_{en} = \exp(0.632 - 0.101\, S^*T^*O^*\dot{\varepsilon}^*\,), \tag{16}$$

for low-alloy steels

$$F_{en} = \exp(0.702 - 0.101\, S^*T^*O^*\dot{\varepsilon}^*\,), \tag{17}$$

for austenitic SSs,

$$F_{en} = \exp(0.734 - T^*O^*\dot{\varepsilon}^*\,), \tag{18}$$

and for Ni-Cr-Fe alloys,

$$F_{en} = \exp(-T^*O^*\dot{\varepsilon}^*\,). \tag{19}$$

In NUREG-6909, rev 1 [16], the fatigue ε–N data were re-analyzed for both carbon and low-alloy steels with a different dependence (of fatigue life) on strain rate, DO, and temperature. A single F_{en} expression was developed for both carbon and low-alloy steels,

$$F_{en} = \exp((0.003 - 0.031\dot{\varepsilon}^*)\, S^* T^* O^*). \tag{20}$$

For austenitic SSs and Ni-Cr-Fe alloys, after re-analyzing with additional data, Eq. (19) was used for the F_{en} expression in NUREG-6909, rev 1. Table 2 summarize the assigned values of the transformed parameters $S^*, T^*, O^*,$ and $\dot{\varepsilon}^*$.

Table 2. Transformed parameters $S^*, T^*, O^*,$ and $\dot{\varepsilon}^*$ for carbon and low-alloy steels, austenitic SS, and Ni-Cr-Fe alloys

Transformed parameters	Carbon and low-alloy steels		Austenitic SS		Ni-Cr-Fe alloys	
	value	condition	value	condition	value	condition
S*	2.0+98*S	S≤0.015, %	-	-	-	-
	3.47	S>0.015, %	-	-	-	-
T*	0.395	T<150°C	0	T<100°C	0	T<50°C
	(T-75)/190	150 ≤ T ≤ 325°C	(T-100)/250	100 ≤T ≤ 325°C	(T-50)/275	50 ≤T ≤ 325°C
O*	1.49	DO<0.04ppm	0.29	DO<0.1ppm	0.14	DO<0.1ppm
	ln(DO/0.009)	0.04≤DO≤0.5ppm	0.29	DO≥0.1ppm, sensitized SSs	-	-
	4.02	DO>0.5ppm	0.14	DO≥0.1ppm	0.06	DO≥0.1ppm
$\dot{\varepsilon}^*$	0	$\dot{\varepsilon} > 2.2\%/s$	0	$\dot{\varepsilon} > 7\%/s$	0	$\dot{\varepsilon} > 5\%/s$
	ln($\dot{\varepsilon}$/2.2)	$0.0004\%/s \le \dot{\varepsilon} \le 2.2\%$	ln($\dot{\varepsilon}$/7)	$0.0004\%/s \le \dot{\varepsilon} \le 7\%$	ln($\dot{\varepsilon}$/5)	$0.0004\%/s \le \dot{\varepsilon} \le 5\%$
	ln(0.0004/2.2)	$\dot{\varepsilon} < 0.0004\%/s$	ln(0.0004/7)	$\dot{\varepsilon} < 0.0004\%/s$	ln(0.0004/5)	$\dot{\varepsilon} < 0.0004\%/s$

Using the approach detailed in NUREG-6909, rev 1, environmental effects on the fatigue performance of reactor materials can be assessed with F_{en}, providing a technical basis for evaluating the usage of reactor components in service operation. This approach relies on the experimental data obtained from small, smooth samples tested in LWR coolant environments, and predicts the remaining fatigue lives under the covered environmental and loading conditions.

3. Variables influencing fatigue and environmentally assisted fatigue

Experimental variables influencing fatigue and EAF can be broadly classified into three groups -- material, loading, and environment. Within each group, additional subcategories can be identified [15].

Material
  (i)   Composition
  (ii) Metallurgy -- grain size, inclusions, orientation within a forging or plate
  (iii) Manufacturing and processing conditions -- cold work, solution annealed etc.
  (iv) Size and geometry
  (v)   Surface finish: fabrication surface condition
  (vi) Surface preparation: surface work hardening
Loading
  (i)   Strain rate -- rise time
  (ii) Sequence of varying stress -- linear damage summation or Miner's rule
  (iii) Mean stress and hold time
  (iv) Biaxial effects -- crack tip constraint
Environment
  (i)   Water chemistry -- DO, lithium hydroxide, boric acid concentrations
  (ii) Temperature
  (iii) Flow rate

The underlying mechanisms relating these experimental variables to fatigue performance are complex and often are not fully understood. The dependencies of fatigue performance on these variables may arise from the physical and chemical interactions within materials (e.g., effects of sulfur or DO), or from the continuum mechanics of material behavior (e.g., effects of mean stress or biaxial stress). Nonetheless, fatigue test results inherently include these effects. As a result, simple ε-N models, as shown in Eqs. (8) and (14), can capture the influence of these variables and help in extending the laboratory data to component applications.

3.1 Effect of Sulfur Content in Carbon and Low-alloy Steels

Under the category of material composition, sulfur content is the most important factor for carbon and low-alloy steels. Some high-sulfur steels exhibit poor fatigue properties in certain orientations because of the distribution and morphology of sulfides in the steel. In the orientation with poor fatigue resistance, crack propagation occurs preferentially along the sulfide stringers and is facilitated by sulfide cracking.

In LWR environments, sulfur content and morphology become the dominant factor for the EAF of low-alloy steels. A critical concentration of S^{2-} or HS^- ions is needed at crack tips for environmental fatigue to occur. The fatigue crack growth rate and threshold stress intensity factor are both a function of the sulfur content up to 0.019 wt.%. Below 0.005 wt.%, the fatigue crack growth rate of low-alloy steels in LWR environment declines considerably, suggesting a strong

effect of sulfur. The available datasets are insufficient to establish a dependence of fatigue lives on sulfur content and to accurately define the threshold value for sulfur effect. Nonetheless, fatigue lives of carbon and low-alloy steels are assumed to saturate at a sulfur content of 0.015 wt.%. Additional data with high sulfur content would help validate the assumption.

3.2 Effect of Temperature

3.2.1 Carbon and low-alloy steels

Temperature is one of the most important parameters influencing the deformation behavior of materials. For carbon and low-alloy steels, a higher lattice friction force is expected with decreasing temperature, which can influence the development of fatigue damage. It was found that, without water environment, the fatigue lives of carbon and low-alloy steels decrease with temperature [16]. The existing data on multiple heats of carbon and low-alloys steels illustrates a moderate effect of temperature, and the resulting reduction factor is less than 1.5 between 25°C and 290°C.

Figure 3 shows the fatigue life in water as a function temperature at different levels of DO and strain rates. A temperature threshold can be seen with the LWR environment. Above ~150°C, the LWR environment with a DO level higher than 0.05 ppm reduces fatigue life. The extent of decrease was greater at higher temperatures. It is clear that the effects of temperature on the EAF of carbon and low-alloy steels in LWR environments can be evaluated with F_{en} whose expression is given in Eq. (20).

Figure 3. Environmental fatigue of carbon and low-alloy steels as a function of temperature [16]

8

3.2.2 Austenitic SSs and Ni-Cr-Fe alloys

For austenitic SSs, the existing data without environment does not show any dependence on temperature from room temperature up to 400°C. Limited data between 427 and 456°C also shows no temperature effect. It is evident that, without environment, temperature has no effect on the fatigue performance of SSs.

With LWR environment however, a threshold behavior is again observed as shown in Figure 4. Above ~100°C, fatigue lives of SSs decrease with temperature. Furthermore, the effect of temperature seems to be affected by strain rate. For a high strain rate (i.e., 0.4%/s), the effect of temperature is not clear. Nevertheless, if the strain rate is lowered to 0.01%/s, the influence of temperature on fatigue lives becomes obvious. This suggests that LWR environment is the true origin of the observed temperature dependence of fatigue life. A strain rate too high would not allow for sufficient interaction between the sample and environment. This observation further confirms that the temperature effect in austenitic SSs stems from its impact on LWR environment.
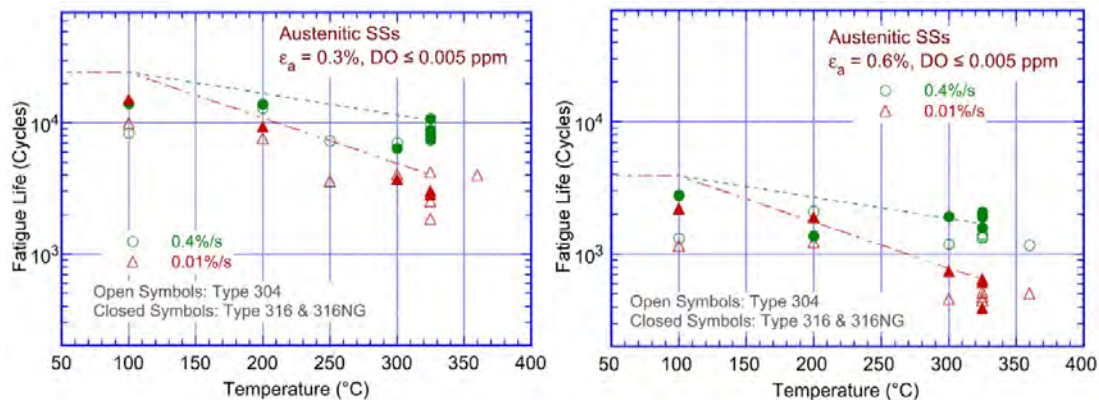
Figure 4. Fatigue life of austenitic SSs as a function of temperature in LWR environment [16]

Limited amount of fatigue data is available for other Ni-Cr-Fe alloys, such as Alloys 600 and 690. The best-fit air curve for austenitic SSs, which is consistent or conservatively bounding the Ni-alloys data, is used to describe the fatigue behavior of Ni-Cr-Fe alloys. With LWR environment, the same approach as that used for austenitic SSs can be taken. The threshold value has also been conservatively lowered to 50°C.

3.3 Effect of Strain Rate

3.3.1 Carbon and low-alloy steels

Strain rate is not typically modeled in fatigue without environment. It was found that some heats of carbon and low-alloy steels were sensitive to strain rate while the others were not [17]. The reason for this inconsistency is not clear, but the effect of strain rate seems to depend on steel's carbon and nitrogen contents and the occurrence of dynamic strain aging (DSA). Localized plastic flow associated with DSA may influence the crack tip stress-strain field, leading to a complex

dependency on strain rate. Consequently, the effect of strain rate on fatigue life without environment is accounted for by the subfactor of data scatter and materials variability.

With LWR environment, the situation is completely different. The effect of strain rate on the fatigue lives of carbon and low-alloy steels is significant. When other conditions for EAF are satisfied (e.g., strain amplitude, temperature, and DO content), fatigue life declines considerably with the decrease of strain rate as shown in Figure 5 (the green lines). Using F_{en}, the effect of strain rate can be explicitly modeled. There seems to be a saturation value for the effect of strain rate as well, since at very low strain rates, fatigue may not be the dominant damage mechanism.

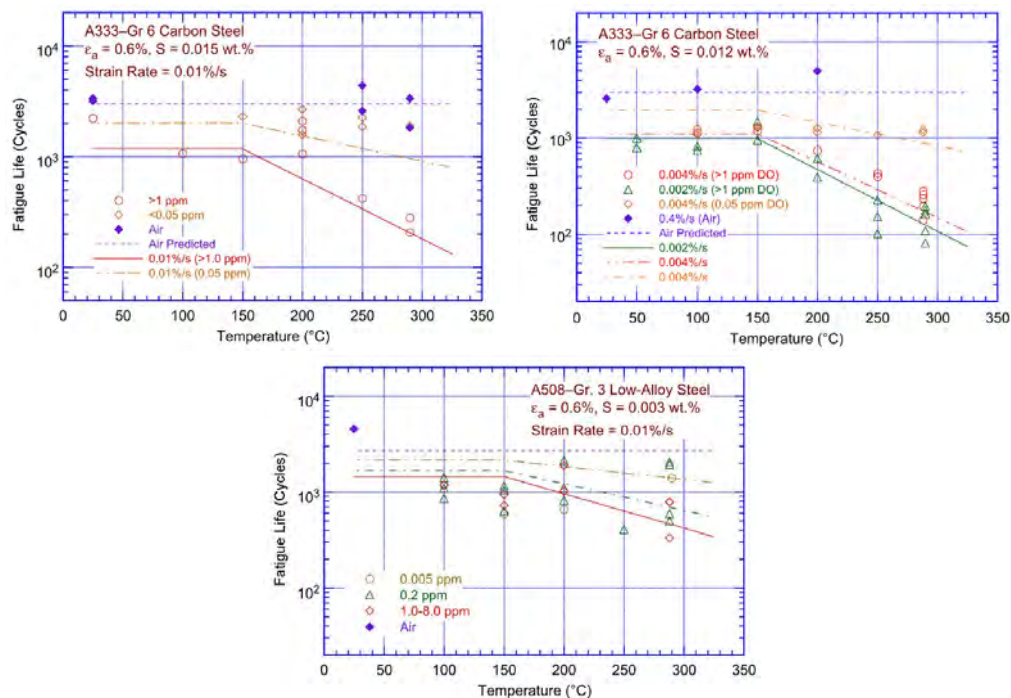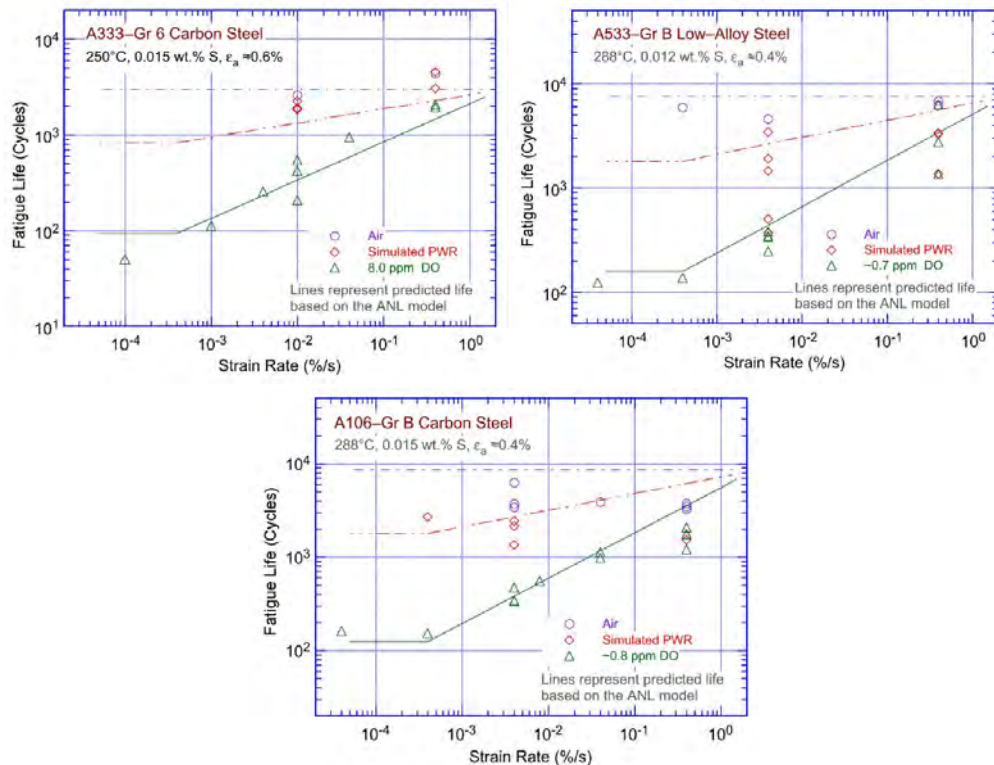

Figure 5. Fatigue lives of carbon and low-alloy steels as a function of strain rate [16]

3.3.2 Austenitic SSs and Ni-Cr-Fe alloys

For austenitic SSs, no consistent effect of strain rate on fatigue life can be observed without environment. With environment however, a similar dependence of fatigue life on strain rate can be seen as shown in Figure 6. An analysis of a larger database suggests that, below 7%/s strain rate, the fatigue lives of austenitic SSs decrease with decreasing strain rates in low-DO environments. In high-DO water at 288°C, the effects of strain rate are less pronounced than that in low-DO water. Evidently, the effect of strain rate is a variable relevant specifically to EAF.

With limited data available for Alloys 600 and 690, a similar decreasing trend of fatigue life with decreasing strain rate can be observed in Figure 7. The analysis also shows that the threshold value for strain-rate effect decreases from 7%/s for austenitic SSs to 5%/s for Ni alloys.
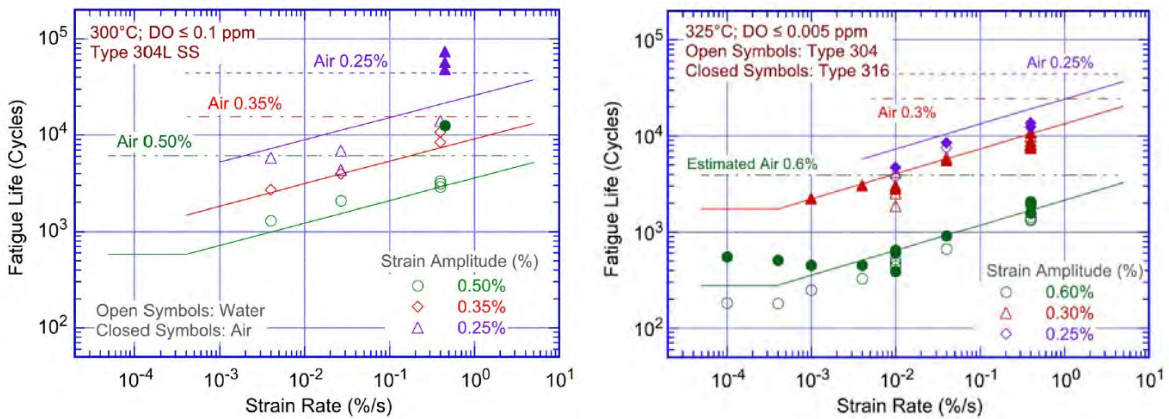
Figure 6. Fatigue lives of austenitic SSs as a function of strain rate [16]
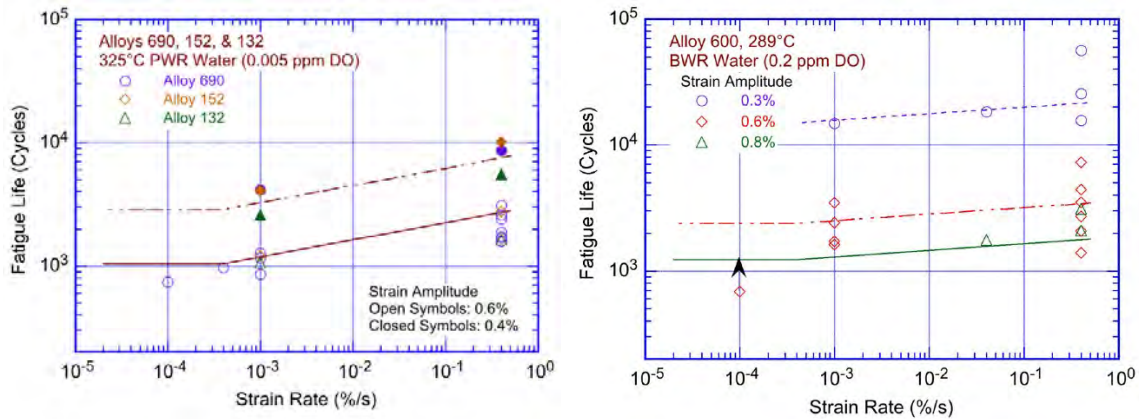
Figure 7. Fatigue lives of Alloy 600 and 690 as a function of strain rate [16]

3.4 Effect of Cyclic Strain Hardening Behavior

3.4.1 Carbon and low-alloy steels

Depending on the processing condition and initial microstructure, carbon and low-alloy steels can experience either cyclic strain hardening, or cyclic strain softening followed by a steady-state period. As shown in Figure 8, carbon steels exhibit significant initial hardening. Low-alloy steels show little or no initial hardening and may exhibit cyclic softening with continued cycling. For both steels, cyclic stresses are higher at elevated temperatures than at room temperature. The extent of hardening increases as the applied strain rate decreases. This cyclic hardening behavior could affect the endurance limit of fatigue without environment. While cyclic hardening does not have a direct link with environmental fatigue, it does affect the stress-strain response, and therefore can influence environmental fatigue indirectly.
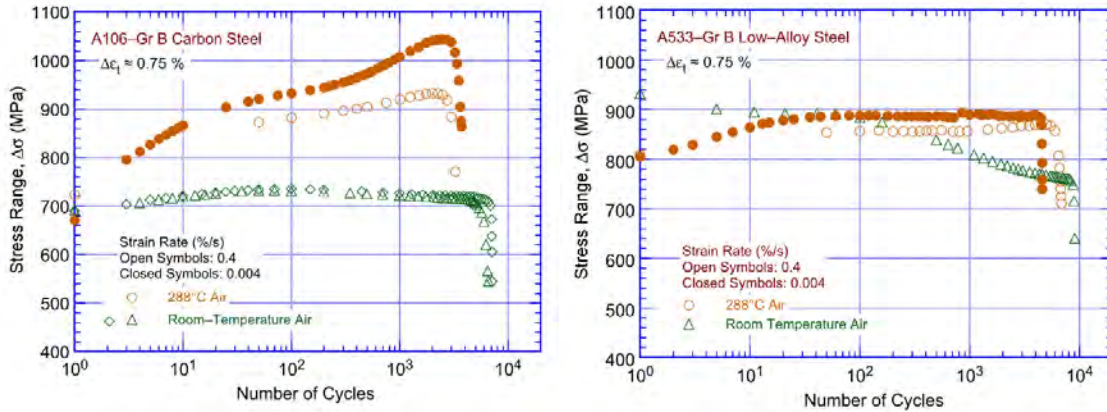
Figure 8. Cyclic strain hardening and softening of carbon and low allow steels [16]

3.4.2 Austenitic SSs and Ni-Cr-Fe alloys

Austenitic SSs exhibit rapid hardening during the initial 50 to 100 cycles, as shown in Figure 9. The extent of hardening increases with increasing strain amplitude and decreasing temperature and strain rate. As a result, cyclic hardening can influence the fatigue lives of SS materials, and the effect can be accounted for by varying the stress in the fatigue model.
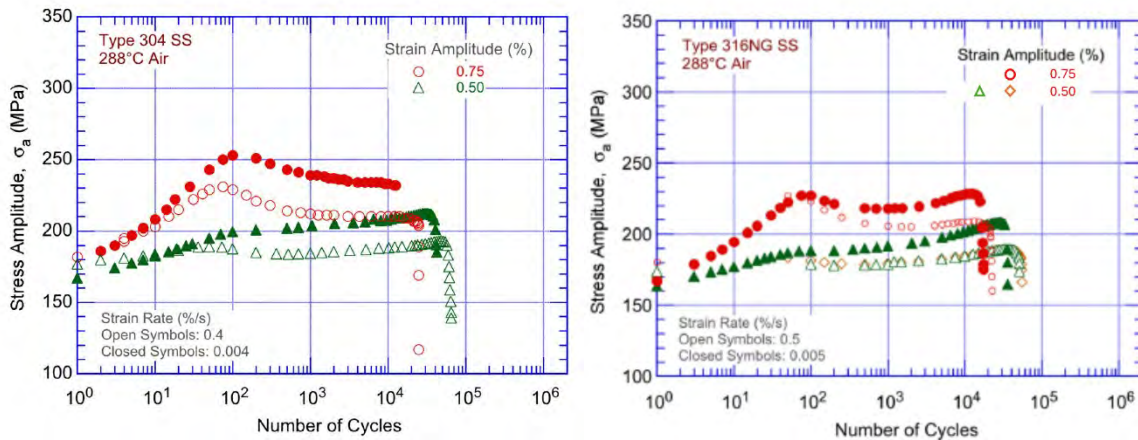
Figure 9. Cyclic hardening of austenitic SSs [16]

3.5 Effect of Surface Finish

3.5.1 Carbon and low-alloy steels

Fatigue life is sensitive to surface finish. A study of the effect of surface finish on the fatigue lives of carbon steels showed a factor of 2 decrease in life when average surface roughness (Ra) was increased from 0.3 to 5.3 µm [18]. The effect of surface finish is one of the reasons behind the difference in fatigue lives between laboratory specimens and reactor components. For an actual component with an industrial-grade surface finish, cracks can initiate at surface irregularities that are normal to the axis of applied stress. The height, spacing, shape, and distribution of surface irregularities are important for crack initiation. As shown in Figure 10, the fatigue life of a carbon

12

steel with an intentionally roughened surface is about a factor of 3 lower than those of smooth samples. This is consistent with the other observations that fatigue lives decrease as surface roughness increases.
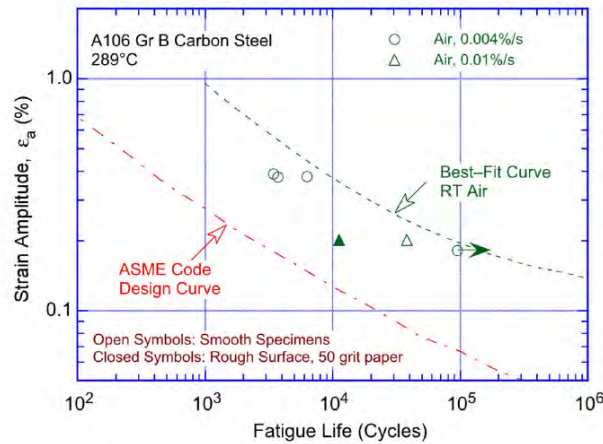
Figure 10. Fatigue lives in air of carbon steels with different surface finish [16]

In LWR environments, a similar effect of surface finish can be seen. As shown in Figure 11, for both carbon and low-alloy steels, the samples with rough surfaces have lower fatigue lives and are close to the ASME design curves. This suggests that the reduction factor due to surface roughness is about the same as that of in air tests.
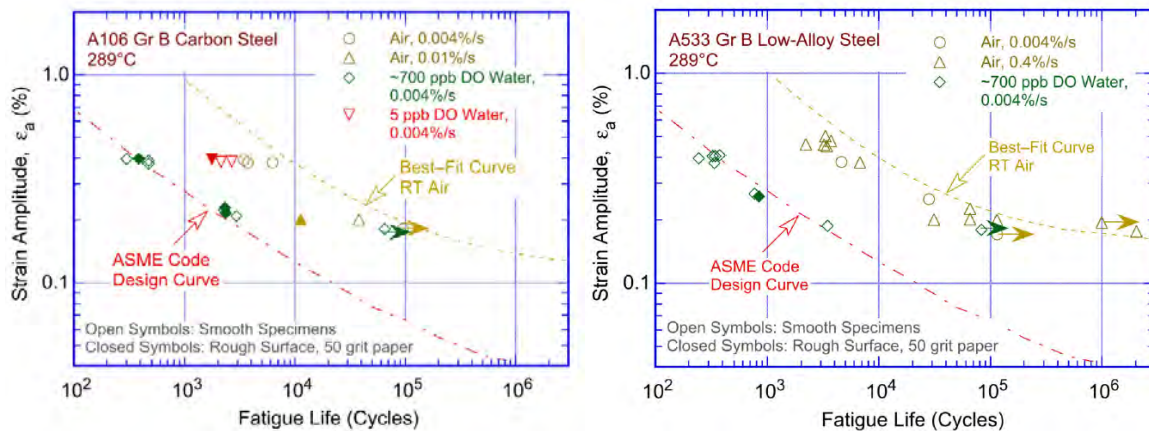
Figure 11. Environmental fatigue of carbon and low-alloy steels with different surface finish [16]

3.5.2 Austenitic SSs and Ni-Cr-Fe alloys

Studies on austenitic SSs for the effect of surface roughness show a similar reduction in fatigue life in air for austenitic SSs [21][22]. The fatigue life for crack initiation (N_i) was found to be related to the root-mean-square roughness[2] (R_q) by $N_i = 1012 \, R_q^{-0.21}$. This would lead to a factor of 3

---

[2] Note that R_Q is the root-mean-square average of the roughness profile ordinates.

13

reduction in fatigue life when the R_q is measured in micrometers, consistent with what observed in fatigue tests on austenitic SSs without environment.

With LWR environment, Figure 12 shows the EAF results. The fatigue lives of the rough samples are slightly lower than those of smooth samples tested in water environment. With the environment, the reduction factor attributing to surface roughness is generally less than 3, and sometime even smaller [16]. This observation indicates that the impact of surface finish is not an environment-only effect, and should be included in the fatigue design curve without environment.
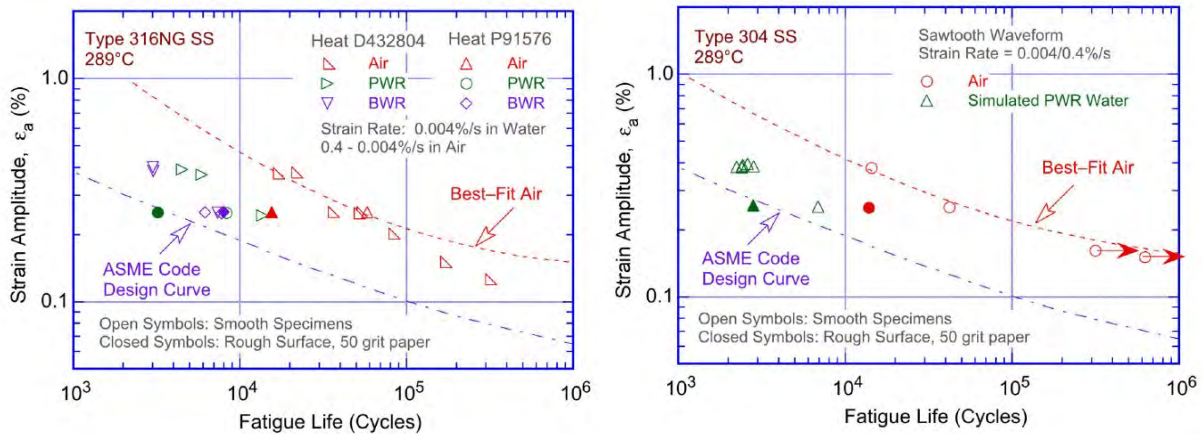
Figure 12. Environmental fatigue of austenitic SSs with different surface finish [16]

3.6 Effect of Dissolved Oxygen

Dissolved Oxygen is a key water chemistry parameter influencing fatigue performance under the category of "environment". As shown in Figure 13, the fatigue life of carbon steels dropped significantly with the increasing DO level. The effect of DO is less evident in low-alloy steels. The difference was attributed to the crack tip chemistry, which is linked to the detrimental effect of sulfur on environmentally enhanced crack growth [16].
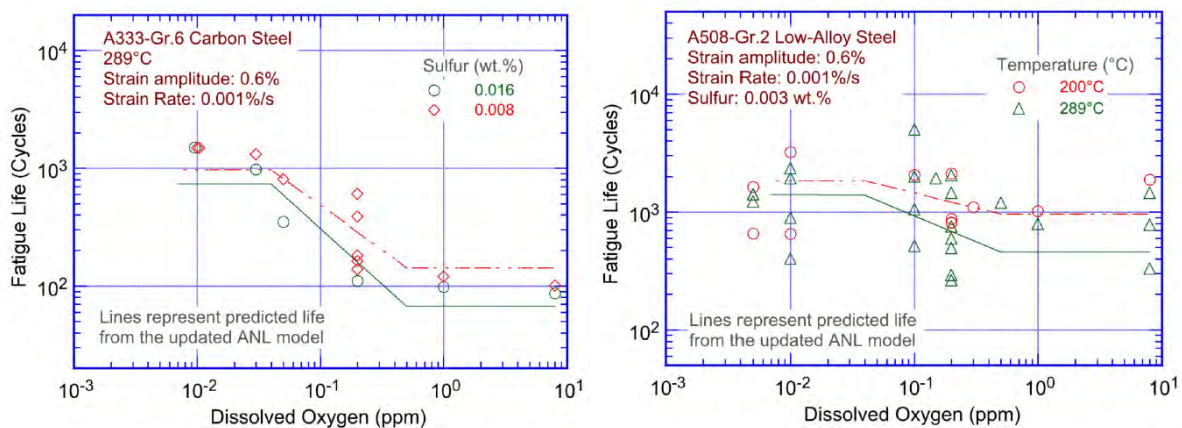
Figure 13. Environmental fatigue of carbon and low-alloy steels as a function of dissolved oxygen level [16]

14

For austenitic SSs, the fatigue life decreases significantly in low-DO water (i.e., < 0.05 ppm DO). In low-DO water, fatigue lives are not influenced by the material composition or heat treatment. The fatigue lives, however, do decrease with decreasing strain rate and increasing temperature. In high-DO water, the fatigue lives of austenitic SSs are comparable or higher than those in low-DO environment as shown in Figure 14. Material composition or sensitization may affect the fatigue response more strongly than DO level. Nonetheless, the effect of DO can be captured with the F_{en} approach.
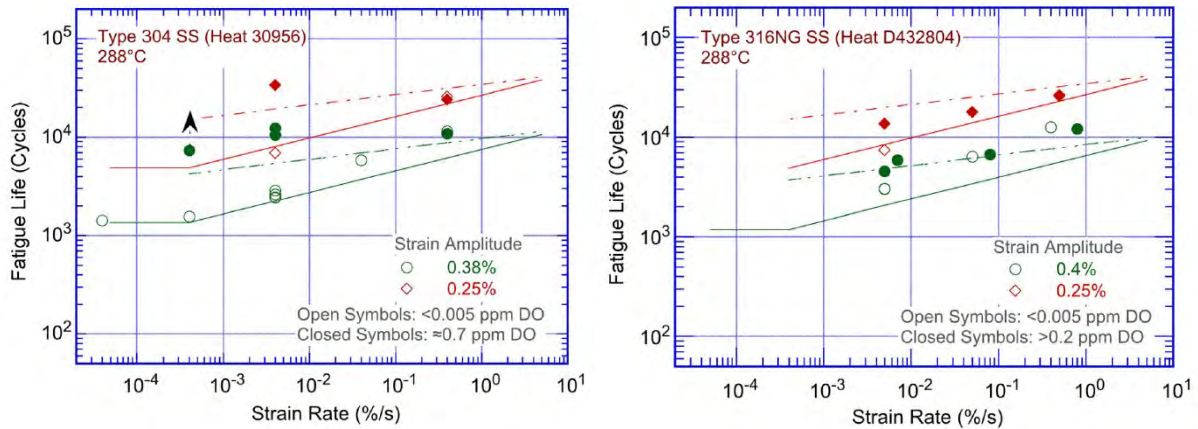
Figure 14. Environmental fatigue of austenitic SSs in low- and high-DO water as a function of strain rate [16]

3.7 Effect of Hold Time

Fatigue tests conducted using trapezoidal loading waveforms indicated that hold times at peak tensile strains decreased the fatigue lives of carbon steels in high-DO water at 289°C. A 300-sec hold period was sufficient to reduce fatigue lives by approximately 50%. A longer hold time of 1800 s reduced fatigue lives further in carbon steels. Figure 15 shows the change in fatigue life with hold time for a carbon steel. The reductions in fatigue lives were attributed to slow strain rates during the hold periods.

For austenitic SSs, the available data did not demonstrate a hold-time effect. Hold at peak tensile strains did not affect the fatigue lives of austenitic SSs in LWR environments. In high-DO water, the fatigue lives obtained with a trapezoidal waveform were comparable to those tested with a triangular waveform. The results indicated little or no effects of hold time at peak tensile strains on the fatigue lives of austenitic SSs. For this reason, there is no need to include the hold-time effect in the F_{en} approach.
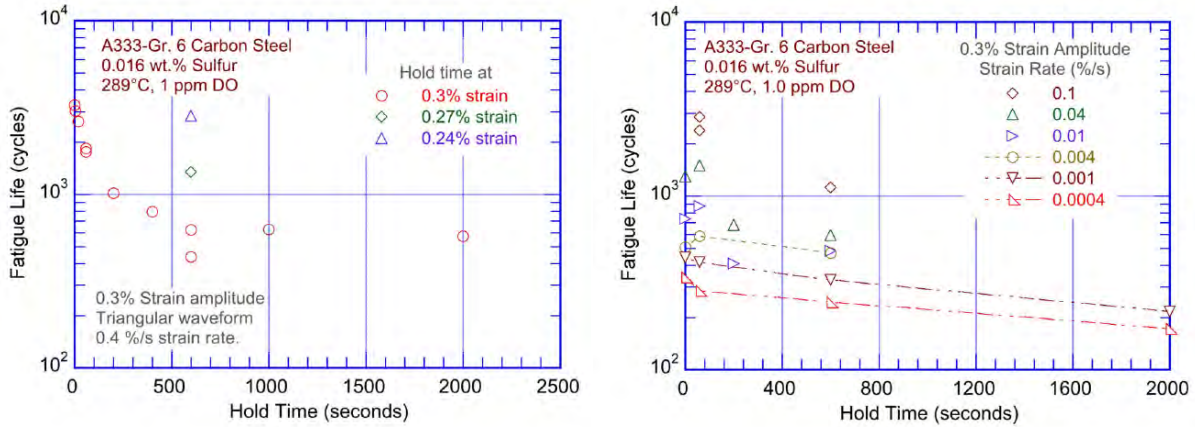
Figure 15. Effect of hold time on the environmental fatigue of carbon steel [16]

In addition to the effects discussed above, other influential variables related to materials, loading, and environment also contribute to fatigue or EAF to varying degrees. The impacts of these variables are represented by the fitting parameters in the models (e.g., Eqs. 8, 14, or 20). However, de-convoluting their individual effects is challenging because these parameters are often interrelated rather than independent, complicating the analysis of their specific effects on fatigue performance.

4. Component-level EAF Modelling and Predictions

Starting from a rich background in theoretical and experimental EAF, the program was focused on component fatigue prediction and made several major and fundamental contributions in this area. These accomplishments help meet the needs identified by industry relating to component level fatigue predictions in complex, transient conditions [28]. The research discussed in this section describes a system-level finite element (FE) model of reactor coolant system (RCS) components of a pressurized water reactor (PWR). This is with the goal of predicting the stress hotspots, strain residuals, strain amplitudes and the resulting fatigue lives. Topics discussed also include the effects of mean stress/strain, EAF response on dissimilar metal welds (DMWs), as well as Digital Twins.

4.1 System-level Finite Element Model of RCS Components in PWR

To estimate the strain profile and associated residual strain at the end of a reactor loading cycle, a system-level, thermal-mechanical stress analysis was performed on the RCS of PWR [23]. The system-level FE model consists of the RPV, part of a steam generator (SG), part of a pressurizer (PRZ), a hot leg (HL), and a surge line (SL). As shown in Figure 18, the model includes detailed nozzle geometry and material properties of different metals to simulate realistic thermal-mechanical stress-strain under connected-system thermal-mechanical boundary conditions. The resulting strain profile was used for first-hand estimation of the fatigue lives of the HL, SL, and their nozzles.
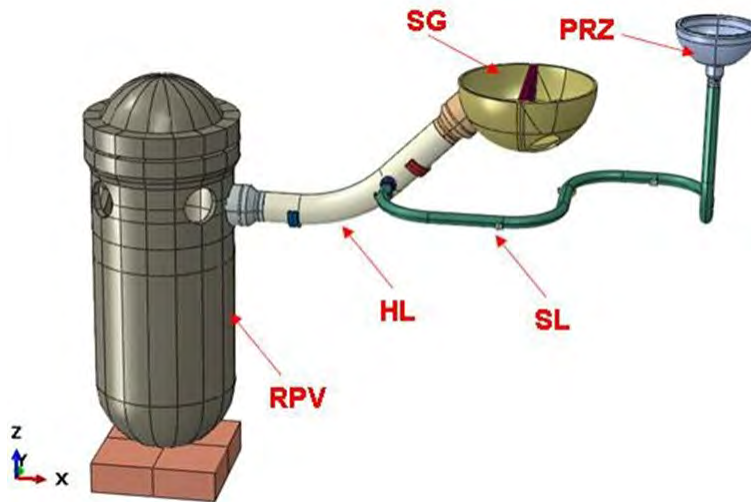
Figure 16. Assembly-level ABAQUS-FE model of RPV [23].

Based on the system-level-FE model, thermal-mechanical stress analysis was performed for a design-basis loading cycle. On the basis of the estimated strain profile, the fatigue lives of the RCS components were estimated. Figure 17 shows an example of maximum principal total and thermal strains at the DMW region of the nozzle. The corresponding strain amplitudes, residual strain, and the fatigue lives are summarized in Table 3. The equivalent or Von-Mises stress amplitude and the corresponding residual (at the end of fuel cycle) values can also be found in Table 3.
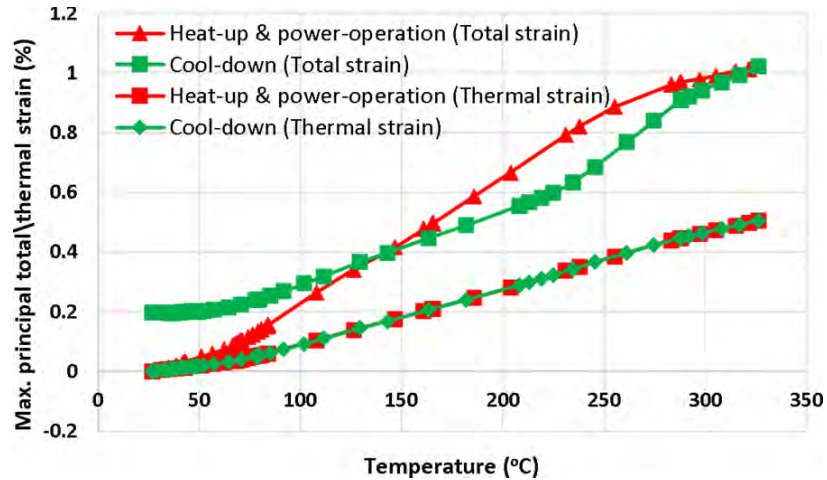
Figure 17. Maximum principal total and thermal strain at the DMW region of the HL-side nozzle of SL [23].

From Table 3, the best case (based on mean curve data) and worse case (based on design curve data) PWR-water-fatigue-life of HL-side nozzle can be 493 and 25 cycles, respectively. These results are representative. The actual life of a particular component can depend on the actual geometry of the component and the plant layout, which governs the connected system thermal-mechanical boundary conditions. Similar results can be obtained for PRZ-side nozzle, SS base pipe region, and SG-side nozzle. Nevertheless, these results show the importance of a system-level model for predicting the stress-strain states and fatigue life of a component. This approach enables more location-specific and accurate fatigue-life predictions compared to relaying on single-component-based simulation models.

Table 3. Summary of various strain, stress amplitudes and estimated of HL-side nozzle of SL.

Parameters	DMW region (if any)	Another region (LAS/SS/SMW) that is more critical than DMW region (if any): SS transition (between DMW and SMW)
Max. of max. principal total strain range (%)	1.021	2.125
Max. of max. principal thermal strain range (%)	0.505	0.498
Max. of equivalent mechanical strain range (%)	0.495	1.672
Max. of equivalent mechanical strain amplitude (%)	**0.248**	**0.836**
Max. of Von Mises stress amplitude (MPa)	356	215
Residual equivalent mechanical strain after 1st cycle (%)	**0.204**	**1.34**
Residual equivalent (Von Mises) stress after 1st cycle (MPa)	175	91
Mean in-air life, N_a (cycles)	49,426	1848
Design in-air life, $N_d = (\frac{1}{20}) * N_a$ (cycles)	2,471	92
Fen	3.75	
Mean PWR water life, $N_w = (\frac{1}{Fen}) * N_a$ (cycles)	13,180	493
Design PWR water life, $N_{w,d} = (\frac{1}{Fen}) * N_d$ (cycles)	659	25
Best case scenario: Mean PWR water life i.e., minimum N_w of all regions (cycles)	**493**	
Worst case scenario: Minimum possible PWR water life i.e., minimum $N_{w,d}$ of all regions (cycles)	**25**	

4.2 Mean Stress or Strain

Mean stress is a subject of interest for fatigue and EAF, since it could be a source of significant uncertainty in fatigue testing and analysis. A good understanding of the mean stress or strain on fatigue performance is crucial for improving the service life prediction and aging management. As we discussed previously, ASME Code and NUREG-6909 are based on fully reverse, strain-controlled tests. In these tests, the same tensile and compressive strain are applied to the sample. The mean strain and strain amplitude are artificially forced to remain constant during the test. Under realistic loading cycles during reactor operation, the mean value of the maximum and minimum strain is not zero. A compressive mean strain (or stress) is beneficial, while a tensile mean strain is detrimental to fatigue life. Currently, a modified Goodman approach (Eqs. 12, 13) is used to correct the fatigue curve to account for the mean-stress effect. While this correction mainly affects the endurance limit, it could influence the low-cycle fatigue behavior as well.

Recognizing the need of better understanding of the realistic loading condition on the fatigue life prediction, Mohanty and coworkers conducted research employing a system-level approach to calculate the thermal and mechanical stress cycles and the evolution of material properties, and developed mechanics models for fatigue life prediction on reactor components [24][25][26][27]. In a study of the fatigue life of dissimilar metal weld specimens [24], thermal-mechanical stress analysis was performed on a nozzle assembly under design-basis loading cycle. With this more realistic loading profile, fatigue tests were performed in both air and PWR water environment. The work demonstrated that, with realistic loading, strain rapidly ratchets and then stabilizes. In PWR water, environment affects the mean strain, leading to faster ratcheting of strain.

A detailed comparison of fatigue lives for specimens tested in air and in PWR water environment was provided. As shown in Figure 18, the mean strain does not stay steady under realistic reactor loading as they do in strain-controlled tests. Consequently, ratcheting of strain takes place in water environment. A clear distinguish can be seen between the actuator-position profile, a quantity related to the main strain, between the in-air and in-water tests. The study also showed that the effect of environment on fatigue can be tracked experimentally with ratcheting strain or strain amplitude. Nonetheless, the study concludes that strain-controlled test data does not fully capture the actual behavior of reactor materials under realistic loading conditions, advocating for more detailed strain tracking for low-cycle fatigue evaluation.
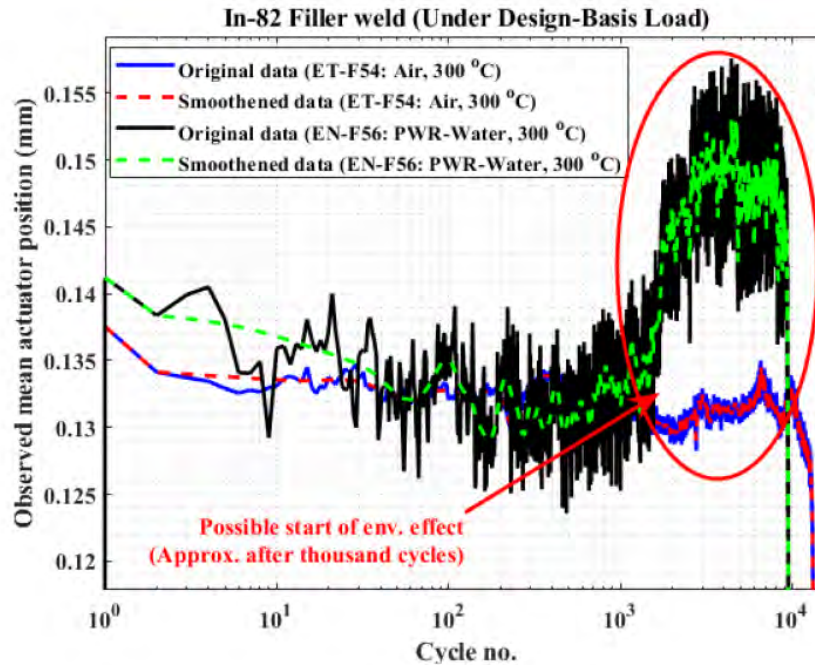
Figure 18. Comparison of the mean actuator-position for an in-air and in PWR-water fatigue tests [24].

4.3 Dissimilar Metal Weld Fatigue Tests

In order to assess the performance of dissimilar metal weld (DMW) in PWR environment, multiple 82/182 DMW specimens, both solid-weld and joint-weld representing the reactor's multi-metal nozzles, were fatigue tested [26]. The tests were primarily conducted under a direct strain-controlled condition except two tests being conducted under a pseudo-strain-controlled condition. All the tests were conducted with a strain rate of 0.01%/s and for different strain amplitudes of 0.3, 0.4, 0.5 and 0.6 %. The resulting fatigue lives were compared to the NUREG-6909 based best-fit and design fatigue curves as shown in Figure 19. The results of 52/152 DMW fatigue specimens tested under an INERI program were also compared to the NUREG-6909 fatigue curves.

Most of the test data fall significantly below the NUREG-6909's best-fit curve in air or the air mean curve, which was established with austenitic SS data due to lack of nickel alloy data. This may require a higher scaling factor (e.g., ASME suggested factor of 20 on cycles rather than the current NUREG-6909 suggested factor of 12 on cycles) for adjusting the austenitic-stainless-steel best-fit-curve for estimating the design or safe-life of a welded component. Based on this assessment, if a DMW component experiences a strain amplitude of 0.6% in the PWR-water, the life of the component would be 52 cycles instead of 85 cycles. However, more DMW tests are required to further ascertain the above-mentioned observations.
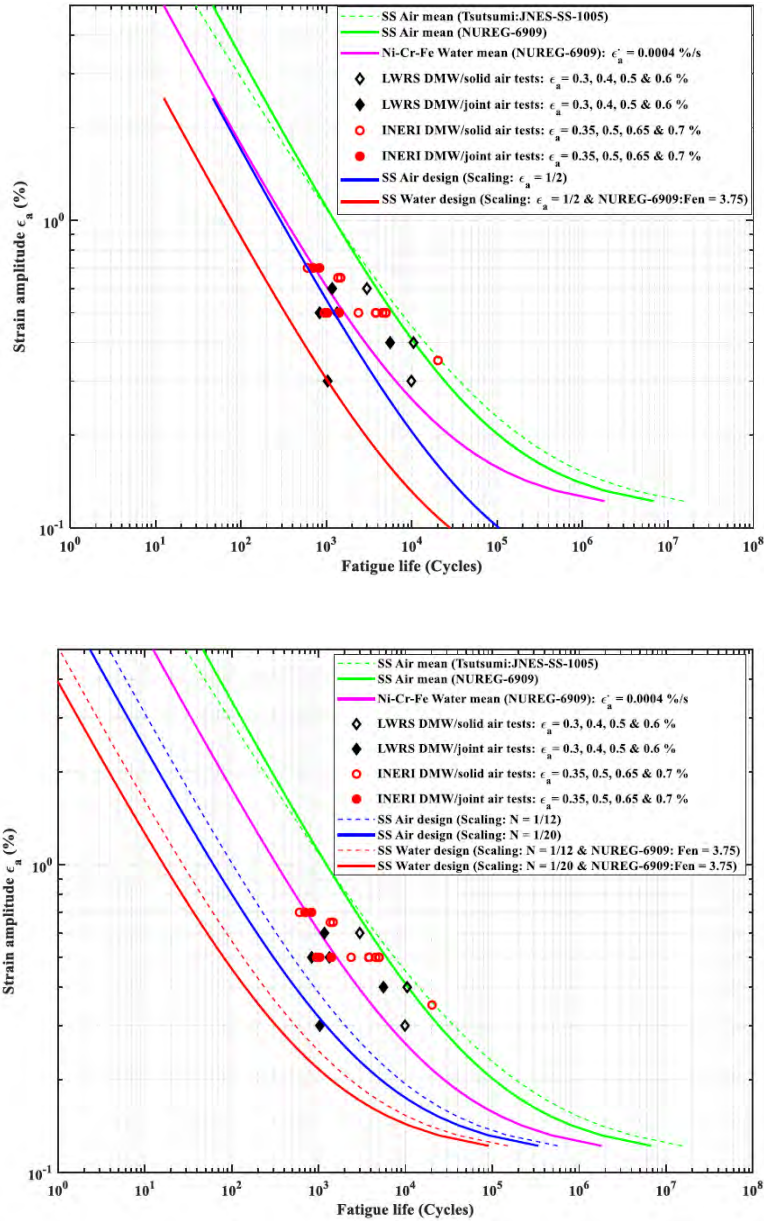
Figure 19. Test data compared with the NUREG-6909 best-fit and design curves.

4.4 Digital Twin Framework for PWR Components

To ensure the safe operation of reactor components, ANL developed a digital twin (DT) framework to predict the structural states and associated fatigue life of components in real-time [26][27]. This framework is a comprehensive system designed to predict the structural states and fatigue lives of reactor components. It includes multiple models that work together to simulate and predict various conditions and behaviors of reactor components under different operational scenarios. The DT framework integrates AI, ML, and FE based modeling tools to evaluate the structural states and fatigue lives.

As shown in Figure 20, the components of the DT framework include real-time process measurements from existing thermal-hydraulic or plant process sensors, AI/ML algorithms for predictive modeling, and physics-based models that simulate the behavior of reactor components under various thermal-mechanical stresses. The framework aims to predict temperature, stress, and strain at any given time and location within the modeled components. In addition to providing the information about the thermal and mechanical states of the modeled components, the DT framework can also be used to predict the cumulative usage factors (CUFs) of reactor components at any given points in the model. Without running FE models in real-time, equivalent fatigue lives at multiple points can be assessed, enhancing the efficiency and accuracy of life estimation for critical reactor components.
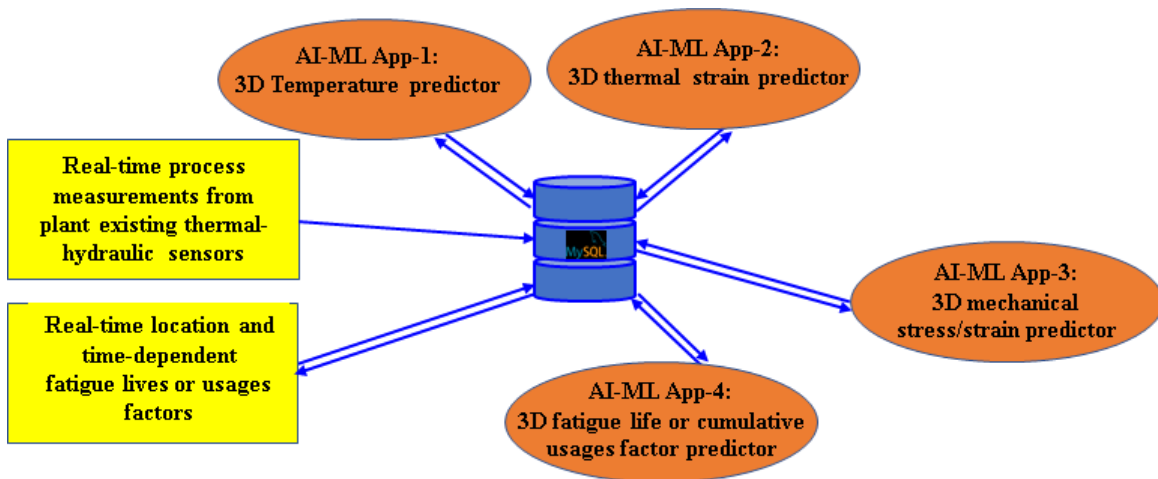
Figure 20. Schematic of data-driven DT framework based on AI-ML with different physics apps and dataflow directions [27]

An example of the DT framework's application is to assess the structural states and fatigue damage of PWR RCS components under a set of connected-system thermal-mechanical boundary conditions [27]. A system-level FE model was developed to simulate the thermal and mechanical strain profiles and associated fatigue lives of a PWR HL, SL, and their DMW-SMW nozzles under connected system thermal-mechanical boundary conditions. The results show some of the RCS components can have significantly less fatigue lives compared to the other components with similar geometry and material. Based on these results, it is surmised that the HL-side nozzle of the SL may be an issue, particularly for long-term operation. Although these results are geometry-specific, one can expect similar qualitative results since most of the power plants have a very similar configuration. Nevertheless, the results obtained from the DT model are representative and can be used as a guideline to inform NDE-related inspections on relevant locations of the RCS.

5. Knowledge Gaps and Future Research Directions

The US DOE LWRS-sponsored research at ANL primarily focused on the EAF response of steels and to a lesser extent weldments in LWR environments. Knowledge gaps include both structural alloys such as steel weldments and Nickel-based alloys and weldments, both conventionally and AM – produced, as well as the response of those alloys in alternative and faulted environments.

For structural steels, EAF research should be expanded to include welds and AM variants (in progress), as well as crack initiation response in faulted environments. The need for additional data, as well as for a standardized methodology for dealing with welds in fatigue design was also recognized by EPRI as an outstanding issue that warrants further investigation [28]. The need for a better understanding of the effect of faulted environments and dissolved oxygen on fatigue crack initiation is a relatively new concern based on the recent French experience with cracking in emergency piping, especially at weld HAZs [29].

EAF research should also attempt to explore whether regulatory conservatism can be reduced by investigating the possibility of occurrence of recovery effects during realistically long hold times [31]-[33]. Concern exists with the prospect that conventional EAF testing in a laboratory does not adequately simulate true operational exposure due to significant deviations in mechanical loading (time-dependent shape of signals) and the sequence of chemical and mechanical load (continuous impact of mechanical and chemical load without hold-times in mechanical load to simulate steady-state conditions) [34]. Previous research suggests that, indeed, it may be possible that long hold-times cause recovery of initial fatigue damage, e.g. by thermal healing of the damaged microstructure or by healing of initial surface damage by corrosion [35], [36]. In essence, the research will explore whether introducing and increasing hold times lead to an increase in fatigue life. This issue was also recognized by the industry as a knowledge gap [28], and its resolution would involve both EAF and corrosion fatigue crack growth and an improved mechanistic understanding of the interaction between the two phenomena.

For Nickel based alloys, some Ni-based weld alloy testing has already been conducted in this program, primarily on Alloys 81/182, research should be expanded to include high Cr alloys such as Alloy 690 and associated Alloy 52/152 weldments. AM variants of Alloy 690 should be included in the test matrix. It is well-known that regulatory acceptance of AM materials is contingent upon their performance in LWR environments [37], [38], and it should be noted that EPRI's International Materials Research (IMR) program identifies testing of AM materials – including SCC and EAF – as a strategic gap [30]. On the weldments, the focus would be on Alloy 52M which has seen widespread use in industry in recent years.

The EAF research on Ni-based alloys (and steels) should also include exploring the use of KOH instead of typical LiOH water chemistry. The research should focus on understanding the effects of KOH on fatigue lives and crack growth rates under cyclic loading. The testing efforts would include both EAF and environmental fatigue crack growth, aiming to develop an improved mechanistic understanding of the interaction between fatigue damage and water chemistry.

Again, we would like to note that EPRI's IMR program identifies the qualification of KOH to control pH in western-style PWRs as another strategic gap [30].

As a more general recommendation, the creation of an EAF database with expert screening – similar to the approach used for SCC of Alloy 600/182 [39][36] and 690/152 [40] – should be considered. A recommendation along similar lines was made by the industry [28].

6. Conclusions

This report summarizes the EAF research conducted at Argonne under the US DOE LWRS program. Starting from a rich background in theoretical and experimental EAF, ANL previously developed an approach to evaluate fatigue performance of reactor materials in light water reactor environments with the correction factor F_{en}. The approach was based on a large body of experimental work performed at Argonne and elsewhere, and was consistent with ASME's methodology governing the design and construction of reactor components. In recent years, the program was focused on component fatigue prediction and made several major and fundamental contributions in this area. These accomplishments help meet the needs identified as by industry relating to component-level fatigue predictions in complex, transient conditions.

The main contribution of the US DOE LWRS program at ANL involved the development of a system-level model for estimating residual strain and fatigue life of nuclear reactor coolant system components under connected-system-thermal-mechanical boundary conditions. Building upon the system-level model, a digital twin (DT) framework was developed to predict the structural states and associated fatigue life of reactor components in real-time. The DT framework included real-time process measurements from sensors, AI/ML algorithms for predictive modeling, and physics-based models for simulating the behavior of reactor components under various thermal-mechanical stresses. Using the system-level model, more realistic strain conditions were implemented in fatigue testing, and the results were compared with those obtained from the more traditional approach of using F_{en}. The work illustrated that strain-controlled test data did not fully capture the actual behavior of reactor materials under realistic loading conditions, and more detailed strain tracking would be needed to simulate the stress-strain condition for low-cycle fatigue evaluation. It was also shown that the results obtained from the DT were representative and could be used to inform NDE-related inspections on relevant locations of the RCS.

REFERENCES

[1] S. Suresh, "Fatigue of Materials," Cambridge University Press,1998

[2] ASME, "Section III, Rules for Construction of Nuclear Facilities Components", ASME Boiler and Pressure Vessel Code, 2015 Edition, The American Society of Mechanical Engineers, New York, July 2015

[3] US NRC, "Generic Aging Lessons Learned Report," NUREG-1801, Rev. 2, 2010

[4] V. N. Shah, P. E. MacDonald, Aging and Life Extension of Major Light Water Reactor Components, Elsevier Press, 1993

[5] O.K. Chopra, A.S. Rao, A review of irradiation effects on LWR core internal materials - Neutron embrittlement, 409(3), pp 235–256, 2011.

[6] Hans-Peter Seifert, Stefan Ritter, Research and Service Experience with Environmentally-Assisted Cracking in Carbon and Low-Alloy Steels in High- Temperature Water, SKI Report 2005:60, Laboratory for Materials Behavior, SWITZERLAND, 2005

[7] B. F. Langer, "Design of Pressure Vessels for Low-Cycle Fatigue," J. Basic Engineering, Sept., 1962, P 389

[8] L. F. Coffin, Jr., "A Study of the Effects of Cyclic Thermal Stresses on a Ductile Metal," Trans. ASME, vol. 76, 1954, p.931

[9] J. F. Tavernelli, and L. F. Coffin, Jr., "A Compilation and Interpretation of Cyclic Strain Fatigue Tests on Metals," Trans. ASM, vol. 51. 1959, p.438.

[10] O. K. Chopra, and Shack, W. J., 1998, "Effects of LWR Coolant Environments on Fatigue Design Curves of Carbon and Low-Alloy Steels," NUREG/CR-6583, ANL-97/18.

[11] O. K. Chopra, and Shack, W. J., 2001, "Environmental Effects on Fatigue Crack Initiation in Piping and Pressure Vessel Steels," Report No. NUREG/ CR-6717, ANL-00/27.

[12] O. K. Chopra, 1999, "Effects of LWR Coolant Environments on Fatigue Design Curves of Austenitic Stainless Steels," Report No. NUREG/CR-5704, ANL-98/31.

[13] O. K. Chopra, and Gavenda, D. J., 1998, "Effects of LWR Coolant Environments on Fatigue Lives of Austenitic Stainless Steels," ASME J. Pressure Vessel Technol., 120(2), p.116.

[14] W. E. Cooper, 1992, "The Initial Scope and Intent of the Section III Fatigue Design Procedure," Workshop on Cyclic Life and Environmental Effects in Nuclear Applications, Welding Research Council, Clearwater, FL, Jan. 21–22.

[15] O. K. Chopra, and W.J. Shack, "Effect of LWR Coolant Environments on the Fatigue Life of Reactor Materials—Final Report," NUREG/CR-6909, ANL-06/08, February 2007.

[16] O. K. Chopra, and G. L. Stevens, "Effect of LWR Coolant Environments on the Fatigue Life of Reactor Materials—Final Report," NUREG/CR-6909. Rev.1, May 2018.

[17] Abdel–Raouf, H., A. Plumtree, and T. H. Topper, "Effects of Temperature and Deformation Rate on Cyclic Strength and Fracture of Low–Carbon Steel," Cyclic Stress–Strain Behavior – Analysis, Experimentation, and Failure Prediction, ASTM STP 519, American Society for Testing and Materials, Philadelphia, pp. 28–57, 1973.

[18] K. Iida, "A Study of Surface Finish Effect Factor in ASME B&PV Code Section III," in

[19] Pressure Vessel Technology, Volume 2, L. Cengdian and R.W. Nichols (eds.),

[20] Pergamon Press, New York, NY, pp. 727–734, 1989.

[21] P.S. Maiya, and D.E. Busch, "Effect of Surface Roughness on Low-Cycle Fatigue Behavior of Type 304 Stainless Steel," Metallurgical Transactions 6A:1761–1766, 1975.

[22] P. S. Maiya, "Effect of Surface Roughness and Strain Range on Low-Cycle Fatigue Behavior of Type 304 Stainless Steel," Scripta Metallurgica 9:1277–1282, 1975.

[23] Mohanty, S. A System-Level Model for Estimating Residual Strain and Life of Nuclear Reactor Coolant System Components Under Connected-System-Thermal–Mechanical Boundary Conditions. *Exp Mech* **62**, 1501–1517 (2022). https://doi.org/10.1007/s11340-022-00847-5

[24] S. Mohanty, J. P. Park, J. T. Listwan, 2019. "A System-Level Framework for Fatigue Life Prediction of PWR Pressurizer-Surge-Line Nozzle under Design-Basis Loading Cycles. A complete tensile test-based material properties database and preliminary results on 3D weld process modeling, thermal-mechanical stress analysis and environmental fatigue testing", Report No. ANL-LWRS-19/01, Argonne National Laboratory.

[25] Mohanty, S., and Listwan, J., 2020. "A Hybrid AI/ML and Computational Mechanics Based Approach for Time-Series State and Fatigue Life Estimation of Nuclear Reactor Components." Report No. ANL/LWRS-20/01 Argonne National Laboratory.

[26] Mohanty, S., and Listwan, J., 2021. "Development of Digital Twin Predictive Model for PWR Components: Updates on Multi Times Series Temperature Prediction Using Recurrent Neural Network, DMW Fatigue Tests, System Level Thermal-Mechanical-Stress Analysis." Report No. ANL/LWRS-21/02. Argonne National Laboratory.

[27] Mohanty, S., and Listwan, J., 2022. "Hybrid AI-ML and FE-based Digital Twin Predictive Modeling Framework for a PWR Coolant System Components: Updates on Multi-Time-Series-3D-Location Dependent Usages Factor Prediction." Report No. ANL/LWRS-22/1. Argonne National Laboratory.

[28] *Environmentally Assisted Fatigue (EAF) Knowledge Gap Analysis: Update and Revision of the EAF Knowledge Gaps.* EPRI, Palo Alto, CA: 2018. 3002013214.

[29] Whaley, T., Auxiliary Piping Stress Corrosion Cracking Operating Experience Focus Group and Industry Coordination, NRC/Industry Materials Technical Exchange, June 25, 2024, Rockville, MD. ML24173A139

[30] Gift, F., Smith, J., International Materials Research - An Update, NRC/Industry Materials Technical Exchange, June 25, 2024, Rockville, MD. ML24172A291

[31] J Solin, S Reese, H E Karabaki and W Mayinger. Research on Hold Time Effects in Fatigue of Stainless Steel - Simulation of Normal Operation Between Fatigue Transients. Boston, USA: ASME 2015 Pressure Vessels and Piping Conference PVP2015, July, 2015. PVP2015-45098.

[32] J Solin, S Reese and W Mayinger. Long Life Fatigue Performance of Stainless Steel Discussion on Fatigue Design Curves for Stainless Steels. Baltimore, USA: ASME 2011 Pressure Vessels and Piping Conference PVP2011, July, 2011. PVP2011-57942.

[33] E Karabaki, M Twite, J Solin, M Herbst, J Mann and G Burke. Fatigue Performance of Stainless Steels (304L, 347) In Experiments Simulating NPP Operation Hold Times. Vancouver, USA: ASME 2016 Pressure Vessels and Piping Conference PVP2016, July, 2016. PVP2016-63115.

[34] A Roth and B Devrient. Environmental Effects on Fatigue - Possible Reasons for the Apparent Mismatch Between Laboratory Test Results and Operational Experience. Avignon, France: Fontevraud 7, September, 2010. A031-T05.

[35] N Platts, D R Tice, A Panteli and S Cruchley. Effect of Hold Periods on the Corrosion Fatigue Crack Growth Rates of Austenitic Stainless Steels in LWR Coolant Environments. Waikoloa Village, Hawaii: ASME 2017 Pressure Vessels and Piping Conference PVP2017, July, 2017. PVP2017-65787.

[36] H P Seifert, S Ritter and H Leber. *Effect of Static Load Hold Periods on the Corrosion Fatigue Behaviour of Austenitic Stainless Steels in Simulated BWR Environments.* Colorado Springs, USA: 15th International Conference on Environmental Degradation of Materials in Nuclear Systems - Water Reactors, August, 2011. No: 0547.

[37] Roadmap for Regulatory Acceptance of Advanced Manufacturing Methods in the Nuclear Energy Industry, Nuclear Energy Institute, May 13, 2019.

[38] A. Hiser, NRC Perspectives on Advanced Manufacturing Technologies, GAIN Advanced Manufacturing for Nuclear Workshop, December 4, 2018.

[39] Materials Reliability Program: Crack Growth Rates for Evaluating Primary Water Stress Corrosion Cracking (PWSCC) of Alloy 82, 182, and 132 Welds (MRP-115), EPRI, Palo Alto, CA: 2004. 1006696.

[40] Electric Power Research Institute, "Recommended Factors of Improvement for Evaluating Primary Water Stress Corrosion Cracking (PWSCC) Growth Rates of Thick-Wall Alloy 690 Materials and Alloy 52, 152, and Variants Welds (MRP-386)," Palo Alto, CA, 2017: 3002010756.

Nuclear Engineering Division

Argonne National Laboratory
9700 South Cass Avenue, Bldg. #208
Lemont, IL 60439

www.anl.gov